# Observer-based robust control for dynamic positioning of large-scale heavy lift vessels

Ye, J.; Roy, Spandan; Godjevac, M.; Baldi, Simone

**DOI**
10.1016/j.ifacol.2019.06.024

**Publication date**
2019

**Document Version**
Final published version

**Published in**
IFAC-PapersOnLine

Available online at www.sciencedirect.com

ScienceDirect

IFAC Papers Online CONFERENCE PAPER ARCHIVE

IFAC PapersOnLine 52-3 (2019) 138–143

# Observer-based Robust Control for Dynamic Positioning of Large-Scale Heavy Lift Vessels

**Jun Ye** * **Spandan Roy** ** **Milinko Godjevac** * **Simone Baldi** ***

* *Maritime and Transport Technology, Delft University of Techonology, 2628CD, Delft, NL (e-mail: j.ye-1@tudelft.nl, mgodjevac@hotmail.com)*

** *Delft Center for Systems and Control, Delft University of Techonology, 2628CD, Delft, NL (e-mail: s.roy-2@tudelft.nl)*

*** *School of Mathematics, Southeast University, Nanjing 210096, China; Delft Center for System and Control, Delft University of Technology, Delft 2628CD, Delft, NL (e-mail: s.baldi@tudelft.nl)*

**Abstract:** With the growing demand of large-scale heavy lift vessels in the deep-sea offshore construction works, high performance of Dynamic positioning (DP) systems is becoming ever crucial. However, current DP systems on board of heavy lift vessels do not consider model uncertainty (typically arising from mooring forces). In this paper, an observer-based robust controller is designed that can tackle model uncertainty in hydrodynamic damping and mooring forces, environmental disturbances as well as can filter out the high-frequency vessel movement. Closed-loop system stability is analytically established in terms of uniformly ultimately boundedness. In addition, several key performance indicators are provided for tuning the performance of the controller. The effectiveness of the proposed control framework is studied in simulation with a crane-vessel system.



*Keywords:* Dynamic positioning, heavy lift vessel, observer, robust control, large-scale systems

## 1. INTRODUCTION

Heavy lift vessels are large-scale systems where 'large' reflects their physical size. These systems are becoming more and more crucial as, with the increasing demand of oil and gas, the ocean exploration and offshore construction is moving gradually from the shallow sea to the deep ocean, which needs the support of Dynamic Positioning (DP) system. A DP system could automatically maintain a vessel's position and heading by using its own propulsion system. Research on the DP system of offshore crane vessels started in the beginning of the $20^{th}$ century. Early studies showed that the stability of the crane-vessel combination is difficult to obtain with traditional PID position control system [1]. In fact, due to the large external forces from the crane wires, the vessel presents large uncertainties and different dynamics as compared to the free floating mode [2–4]. A study from Vorhölter showed that the performance of DP system of a crane-vessel decreases significantly with load mass heavier than 2% of the vessel displacement [5]. Furthermore, lack of precise parametric knowledge of the crane-vessel system makes the control task of DP challenging. In addition to this, the task become more challenging, especially during a mooring mode, due to the hazardous environment and uncertain additional stiffness.

Research on DP system of offshore cranes mainly focused on two aspects: (i) attempting to reduce the overall stiffness within the system by tuning the PID controller or by applying estimated feedforward force [1, 6, 7]; (ii) considering parametric uncertainty in the control design [8–16]. In the second category, [8–11] concentrated only on the uncertainty involved in the crane dynamics, neglecting the effects of variations in the vessel dynamics; whereas, the latter plays a crucial role in the construction work. Therefore, the recent works [12–16] considered parametric uncertainty (e.g., mooring force, damping force) and external disturbance (e.g., crane force and forces due to wind, sea waves and current) at the vessel level.

However, due to limitation in thruster capabilities, high-frequency position and/or velocity feedback cannot be addressed by a DP system. Unfortunately, all the aforementioned works ignored such scenario. Some notable exceptions are the observer-based designs in [17, 18], where, however, crane/vessel uncertainty is completely ignored.

In light of the above discussions, a composite control solution for DP systems that can tackle parametric uncertainty without using high-frequency feedback is missing. Therefore, an observer based robust controller is proposed in this work which is capable of tackling parametric uncertainties (mooring force, hydrodynamic damping force) and external disturbance forces (crane force, wind, sea waves and current). The control framework is designed with only measured position feedback; thus, ill effects of

⋆ This work is financially supported by the program of China Scholarships Council (CSC) with project No. 20167720003


10.1016/j.ifacol.2019.06.024

high frequency velocity feedback is completely eliminated. The proposed design is modular, as it allows the same framework to be applicable for mooring and free-hanging phase. The closed-loop system is shown to be Uniformly Ultimately Bounded (UUB), with two important Key Performance Indices (KPIs) being provide in terms of (i) ultimate bound of the position error and (ii) upper bound of the required control effort. The effectiveness of the proposed robust controller is verified using a simulated crane-vessel system under the influence of various uncertainties.

The rest of the paper is organized as follows: Section 2 provides the proposed control strategy while Section 3 details the stability result; the simulation results are provided in Section 4; Section 5 presents concluding remarks and future direction.

The following notations are used throughout this paper: $\lambda_{\min}(\bullet)$ and $||\bullet||$ represent minimum eigenvalue and Euclidean norm of $(\bullet)$ respectively; $\mathbf{I}$ denotes identity matrix with appropriate dimension.

## 2. CONTROLLER DESIGN

A generalized three degrees-of-freedom (DoF) DP system dynamics is considered as [17]

$$\dot{\boldsymbol{\eta}} = \mathbf{J}(\psi)\boldsymbol{\nu}, \tag{1}$$

$$\mathbf{M}\dot{\boldsymbol{\nu}} = -\mathbf{D}\boldsymbol{\nu} - \mathbf{F}\boldsymbol{\eta} + \boldsymbol{\tau} + \mathbf{d}_s, \tag{2}$$

$$\mathbf{J}(\psi) = \begin{bmatrix} \cos(\psi) & -\sin(\psi) & 0 \\ \sin(\psi) & \cos(\psi) & 0 \\ 0 & 0 & 1 \end{bmatrix}, \tag{3}$$

where $\boldsymbol{\eta} = [x, y, \psi]^T$ comprises of north position, east position and heading angle of the ship in earth-fixed coordinate system, respectively; $\boldsymbol{\nu} = [u, v, r]^T$ is the vessel velocity/angular velocity in body-fixed coordinate system; $\mathbf{M} \in \mathbb{R}^{3\times3}$ is the mass/inertia matrix; $\mathbf{D} \in \mathbb{R}^{3\times3}$ is the positive definite hydrodynamic damping matrix; $\mathbf{F}\boldsymbol{\eta}$ denotes the mooring force with $\mathbf{F}$ being the positive definite spring coefficient when the mooring force is simplified as linear spring force; $\mathbf{d}_s \in \mathbb{R}^3$ denotes bounded external disturbances representing the effects of wind, wave and current forces; $\boldsymbol{\tau} \in \mathbb{R}^3$ is the generalized control input. Note that, without loss of generality, we consider $[0, 0, 0]^T$ as desired equilibrium position of the vessel.

Henceforth, for compactness, $\mathbf{J}(\psi)$ will be represented as $\mathbf{J}$, and the system dynamics (1)-(2) is represented as

$$\dot{\boldsymbol{\eta}} = \mathbf{J}\boldsymbol{\nu}, \tag{4}$$

$$\dot{\boldsymbol{\nu}} = -\mathbf{A}_1\boldsymbol{\eta} - \mathbf{A}_2\boldsymbol{\nu} + \mathbf{B}\boldsymbol{\tau} + \mathbf{d}, \tag{5}$$

where $\mathbf{A}_1 \triangleq \mathbf{M}^{-1}\mathbf{F}, \mathbf{A}_2 \triangleq \mathbf{M}^{-1}\mathbf{D}$, $\mathbf{B} \triangleq \mathbf{M}^{-1}$ and $\mathbf{d} \triangleq \mathbf{M}^{-1}\mathbf{d}_s$. Note that $\mathbf{A}_1$ and $\mathbf{A}_2$ are positive definite matrices for a crane vessel.

The system (4)-(5) is considered to be uncertain in the sense that, barring $\mathbf{M}$, precise knowledge of $\mathbf{A}_i$, $i = 1, 2$ and $\mathbf{d}$ is not available. Specifically:

*Assumption 1.* $\mathbf{A}_i$'s can be decomposed into two positive definite matrices $\hat{\mathbf{A}}_i$ and $\tilde{\mathbf{A}}_i$ such that $\mathbf{A}_i = \hat{\mathbf{A}}_i + \tilde{\mathbf{A}}_i$; here $\hat{\mathbf{A}}_i$ is the nominal value and $\tilde{\mathbf{A}}_i$ denotes an unknown perturbation in $\hat{\mathbf{A}}_i$. Let $\Delta\mathbf{A}_i$ and $\Delta\mathbf{d}$ denote the maximum possible ranges of $\tilde{\mathbf{A}}_i$ and $\mathbf{d}$, respectively, and their knowledge is considered to be available for control design.

Based on the fact that a ship's thrusters cannot deliver high frequency commands, an observer-based robust controller is designed as

$$\dot{\hat{\boldsymbol{\eta}}} = -\mathbf{K}\hat{\boldsymbol{\eta}} + \mathbf{K}_1\tilde{\boldsymbol{\eta}} + \mathbf{J}\hat{\boldsymbol{\nu}}, \tag{6}$$

$$\dot{\hat{\boldsymbol{\nu}}} = -\hat{\mathbf{A}}_1\hat{\boldsymbol{\eta}} - \hat{\mathbf{A}}_2\hat{\boldsymbol{\nu}} + \mathbf{B}\boldsymbol{\tau} + \mathbf{K}_2(t)\tilde{\boldsymbol{\eta}}, \tag{7}$$

$$\boldsymbol{\tau} = \mathbf{B}^{-1}\{(\hat{\mathbf{A}}_1 - \mathbf{J}^T)\hat{\boldsymbol{\eta}} - \mathbf{K}_2(t)\tilde{\boldsymbol{\eta}} + (\hat{\mathbf{A}}_2 - \rho - \rho_1(t))\hat{\boldsymbol{\nu}}\}, \tag{8}$$

where $\hat{\boldsymbol{\eta}}$ and $\hat{\boldsymbol{\nu}}$ are the observed (filtered) values of $\boldsymbol{\eta}$ and $\boldsymbol{\nu}$ respectively, and $\tilde{\boldsymbol{\eta}} \triangleq \boldsymbol{\eta} - \hat{\boldsymbol{\eta}}$, $\tilde{\boldsymbol{\nu}} \triangleq \boldsymbol{\nu} - \hat{\boldsymbol{\nu}}$. Further, $\hat{\mathbf{A}}_2, \mathbf{K}, \mathbf{K}_1, \mathbf{K}_2, \rho_1$ and $\rho$ are designed as

$$\lambda_{\min}(\mathbf{K}_1) > ||(1/2\beta)\Delta\mathbf{A}_1^T\mathbf{H}^{-1}\Delta\mathbf{A}_1||, \tag{9}$$

$$\lambda_{\min}(\hat{\mathbf{A}}_2) > ||(3\beta/2)\mathbf{H}||, \tag{10}$$

$$\lambda_{\min}(\mathbf{K}) > ||(1/2\beta)\Delta\mathbf{A}_1^T\mathbf{H}^{-1}\Delta\mathbf{A}_1||, \tag{11}$$

$$\rho > ||(1/2\beta)\Delta\mathbf{A}_2^T\mathbf{H}^{-1}\Delta\mathbf{A}_2|| + ||\Delta\mathbf{d}||, \tag{12}$$

$$\rho_1(t) = \alpha||(\mathbf{K}_1 + \mathbf{K})||||\hat{\boldsymbol{\eta}}||||\tilde{\boldsymbol{\eta}}||, \tag{13}$$

$$\mathbf{K}_2(t) = -\hat{\mathbf{A}}_1 + \mathbf{J}^T(t), \tag{14}$$

where $\alpha > 1$; $\beta$ and $\mathbf{H}$ denote a positive scalar and a positive definite matrix.

*Remark 1.* According to Assumption 1, $\hat{\mathbf{A}}_2$ is defined based on the nominal knowledge of $\mathbf{A}_2$. Therefore, condition (10) provides a selection criterion for $\beta$ and $\mathbf{H}$, which in turn guide to select other gains $\mathbf{K}_1, \mathbf{K}, \rho$ and $\rho_1$ from (9), (11), (12) and (13), respectively.

*Remark 2.* Note that the proposed observer based robust controller (6)-(8) based on position feedback only. The reason is that velocity measurements, in general, are more noisy and it is not always desirable to use them in DP controllers.

## 3. STABILITY ANALYSIS

In this section we first give the stability analysis and then we see how the performance of the controller can be appropriately tuned via key performance indicators. Some preliminary definitions are provided below:

*Definition 1. Globally Uniformly Ultimately Bounded Stability [23]:* System (4)-(5) is globally uniformly ultimately bounded if there exists a convex and compact set $\Upsilon$ such that for every initial condition $(\boldsymbol{\eta}(0), \boldsymbol{\nu}(0))$, there exists a finite $T(\boldsymbol{\eta}(0), \boldsymbol{\nu}(0))$ such that $(\boldsymbol{\eta}(t), \boldsymbol{\nu}(t)) \in \Upsilon$ for all $t \geq T(\boldsymbol{\eta}(0), \boldsymbol{\nu}(0))$.

*Definition 2. Ultimate Bound [23]:* A signal $\phi(\cdot)$ is said to be globally uniformly ultimately bounded (UUB) with ultimate bound $b$ if there exists a positive constant $b$, and for any $a \geq 0$, there exists $T = T(a, b)$, where $b$ and $T$ are independent of initial time, such that $\phi(0) \geq a \Rightarrow \phi(t) \leq b$, $\forall t \geq T$.

*Theorem 1.* Under Assumption 1, the system (4)-(5) employing the controller (6)-(8) remains UUB if, for a given $\beta > 0$ and $\mathbf{H} > \mathbf{0}$, the selection of gain parameters $\mathbf{K}, \mathbf{K}_1, \mathbf{K}_2, \hat{\mathbf{A}}_2, \rho$ and $\rho_1$ satisfies (9)-(14).

*Proof 1.* The theorem is proved using the following Lyapunov function:

$$V(\boldsymbol{\xi}) = V_1(\tilde{\boldsymbol{\eta}}, \tilde{\boldsymbol{\nu}}) + V_2(\hat{\boldsymbol{\eta}}, \hat{\boldsymbol{\nu}}), \tag{15}$$

where $\boldsymbol{\xi} \triangleq [\tilde{\boldsymbol{\eta}}^T\ \tilde{\boldsymbol{\nu}}^T\ \hat{\boldsymbol{\eta}}^T\ \hat{\boldsymbol{\nu}}^T]^T$, $V_1 \triangleq (1/2)(\tilde{\boldsymbol{\eta}}^T\tilde{\boldsymbol{\eta}} + \tilde{\boldsymbol{\nu}}^T\tilde{\boldsymbol{\nu}})$ and $V_2 \triangleq (1/2)(\hat{\boldsymbol{\eta}}^T\hat{\boldsymbol{\eta}} + \hat{\boldsymbol{\nu}}^T\hat{\boldsymbol{\nu}})$.

Using (4)-(7), the observer error dynamics can be formulated as

$$\dot{\tilde{\boldsymbol{\eta}}} = \dot{\boldsymbol{\eta}} - \dot{\hat{\boldsymbol{\eta}}} = \mathbf{J}\tilde{\boldsymbol{\nu}} + \mathbf{K}\hat{\boldsymbol{\eta}} - \mathbf{K}_1\tilde{\boldsymbol{\eta}}, \tag{16}$$

$$\begin{aligned}\dot{\tilde{\boldsymbol{\nu}}} = \dot{\boldsymbol{\nu}} - \dot{\hat{\boldsymbol{\nu}}} = &-\hat{\mathbf{A}}_1\tilde{\boldsymbol{\eta}} - \tilde{\mathbf{A}}_1(\tilde{\boldsymbol{\eta}} + \hat{\boldsymbol{\eta}}) - \hat{\mathbf{A}}_2\tilde{\boldsymbol{\nu}} \\ &- \tilde{\mathbf{A}}_2(\tilde{\boldsymbol{\nu}} + \hat{\boldsymbol{\nu}}) - \mathbf{K}_2\tilde{\boldsymbol{\eta}} + \mathbf{d}.\end{aligned} \tag{17}$$

Utilizing (16)-(17), the following can be achieved

$$\begin{aligned}\dot{V}_1 &= \tilde{\boldsymbol{\eta}}^T(-\mathbf{K}_1\tilde{\boldsymbol{\eta}} + \mathbf{K}\hat{\boldsymbol{\eta}} + \mathbf{J}\tilde{\boldsymbol{\nu}}) - \tilde{\boldsymbol{\nu}}^T(\hat{\mathbf{A}}_2 + \tilde{\mathbf{A}}_2)\tilde{\boldsymbol{\nu}} \\ &\quad - \tilde{\boldsymbol{\nu}}^T(\hat{\mathbf{A}}_1 + \mathbf{K}_2 + \tilde{\mathbf{A}}_1)\tilde{\boldsymbol{\eta}} - \tilde{\boldsymbol{\nu}}^T\tilde{\mathbf{A}}_1\hat{\boldsymbol{\eta}} - \tilde{\boldsymbol{\nu}}^T\tilde{\mathbf{A}}_2\hat{\boldsymbol{\nu}} + \tilde{\boldsymbol{\nu}}^T\mathbf{d} \\ &\leq -\tilde{\boldsymbol{\eta}}^T\mathbf{K}_1\tilde{\boldsymbol{\eta}} - \tilde{\boldsymbol{\nu}}^T\hat{\mathbf{A}}_2\tilde{\boldsymbol{\nu}} + \tilde{\boldsymbol{\eta}}^T\mathbf{K}\hat{\boldsymbol{\eta}} - \tilde{\boldsymbol{\nu}}^T\tilde{\mathbf{A}}_1\hat{\boldsymbol{\eta}} \\ &\quad - \tilde{\boldsymbol{\nu}}^T(\hat{\mathbf{A}}_1 + \mathbf{K}_2 - \mathbf{J}^T + \tilde{\mathbf{A}}_1)\tilde{\boldsymbol{\eta}} - \tilde{\boldsymbol{\nu}}^T\tilde{\mathbf{A}}_2\hat{\boldsymbol{\nu}} + \tilde{\boldsymbol{\nu}}^T\mathbf{d},\end{aligned} \tag{18}$$

where we have used the fact that $\tilde{\mathbf{A}}_2$ is positive definite from Assumption 1. Substituting (14) in (18) yields

$$\begin{aligned}\dot{V}_1 \leq &-\tilde{\boldsymbol{\eta}}^T\mathbf{K}_1\tilde{\boldsymbol{\eta}} - \tilde{\boldsymbol{\nu}}^T\hat{\mathbf{A}}_2\tilde{\boldsymbol{\nu}} + \tilde{\boldsymbol{\eta}}^T\mathbf{K}\hat{\boldsymbol{\eta}} \\ &- \tilde{\boldsymbol{\nu}}^T\tilde{\mathbf{A}}_1\tilde{\boldsymbol{\eta}} - \tilde{\boldsymbol{\nu}}^T\tilde{\mathbf{A}}_1\hat{\boldsymbol{\eta}} - \tilde{\boldsymbol{\nu}}^T\tilde{\mathbf{A}}_2\hat{\boldsymbol{\nu}} + \tilde{\boldsymbol{\nu}}^T\mathbf{d}.\end{aligned} \tag{19}$$

Further, using (6)-(8), the following can be deduced

$$\begin{aligned}\dot{V}_2 &= \hat{\boldsymbol{\eta}}^T(-\mathbf{K}\hat{\boldsymbol{\eta}} + \mathbf{K}_1\tilde{\boldsymbol{\eta}} + \mathbf{J}\hat{\boldsymbol{\nu}}) + \hat{\boldsymbol{\nu}}^T(-(\rho+\rho_1)\hat{\boldsymbol{\nu}} - \mathbf{J}^T\hat{\boldsymbol{\eta}}) \\ &= -\hat{\boldsymbol{\eta}}^T\mathbf{K}\hat{\boldsymbol{\eta}} - (\rho+\rho_1)||\hat{\boldsymbol{\nu}}||^2 + \tilde{\boldsymbol{\eta}}^T\mathbf{K}_1\hat{\boldsymbol{\eta}}.\end{aligned} \tag{20}$$

Given any scalar $\beta > 0$ and a positive definite matrix $\mathbf{H}$, the following relation holds for any two non-zero vectors $\mathbf{z}$ and $\mathbf{z}_1$ [24],

$$\pm 2\mathbf{z}^T\mathbf{z}_1 \leq \beta\mathbf{z}^T\mathbf{H}\mathbf{z} + (1/\beta)\mathbf{z}_1^T\mathbf{H}^{-1}\mathbf{z}_1. \tag{21}$$

Applying (21) to the fourth, fifth and sixth terms of (19) the following relations are obtained:

$$-\tilde{\boldsymbol{\nu}}^T\tilde{\mathbf{A}}_1\tilde{\boldsymbol{\eta}} \leq (\beta/2)\tilde{\boldsymbol{\nu}}^T\mathbf{H}\tilde{\boldsymbol{\nu}} + (1/2\beta)\tilde{\boldsymbol{\eta}}^T\Delta\mathbf{A}_1^T\mathbf{H}^{-1}\Delta\mathbf{A}_1\tilde{\boldsymbol{\eta}}, \tag{22}$$

$$-\tilde{\boldsymbol{\nu}}^T\tilde{\mathbf{A}}_1\hat{\boldsymbol{\eta}} \leq (\beta/2)\tilde{\boldsymbol{\nu}}^T\mathbf{H}\tilde{\boldsymbol{\nu}} + (1/2\beta)\hat{\boldsymbol{\eta}}^T\Delta\mathbf{A}_1^T\mathbf{H}^{-1}\Delta\mathbf{A}_1\hat{\boldsymbol{\eta}}, \tag{23}$$

$$-\tilde{\boldsymbol{\nu}}^T\tilde{\mathbf{A}}_2\hat{\boldsymbol{\nu}} \leq (\beta/2)\tilde{\boldsymbol{\nu}}^T\mathbf{H}\tilde{\boldsymbol{\nu}} + (1/2\beta)\hat{\boldsymbol{\nu}}^T\Delta\mathbf{A}_2^T\mathbf{H}^{-1}\Delta\mathbf{A}_2\hat{\boldsymbol{\nu}}, \tag{24}$$

as $\Delta\mathbf{A}_i$ denote the maximum range of $\tilde{\mathbf{A}}_i$ from Assumption 1. Substituting (22)-(24) in (19), the addition of (19) and (20) yields

$$\begin{aligned}\dot{V} \leq &-\tilde{\boldsymbol{\eta}}^T\{\mathbf{K}_1 - (1/2\beta)\Delta\mathbf{A}_1^T\mathbf{H}^{-1}\Delta\mathbf{A}_1\}\tilde{\boldsymbol{\eta}} \\ &- \tilde{\boldsymbol{\nu}}^T\{\hat{\mathbf{A}}_2 - (3\beta/2)\mathbf{H}\}\tilde{\boldsymbol{\nu}} \\ &- \hat{\boldsymbol{\eta}}^T\{\mathbf{K} - (1/2\beta)\Delta\mathbf{A}_1^T\mathbf{H}^{-1}\Delta\mathbf{A}_1\}\hat{\boldsymbol{\eta}} \\ &- \hat{\boldsymbol{\nu}}^T\{\rho\mathbf{I} - (1/2\beta)\Delta\mathbf{A}_2^T\mathbf{H}^{-1}\Delta\mathbf{A}_2\}\hat{\boldsymbol{\nu}} \\ &- \rho_1||\hat{\boldsymbol{\nu}}||^2 + \tilde{\boldsymbol{\eta}}^T(\mathbf{K}+\mathbf{K}_1)\hat{\boldsymbol{\eta}} + \tilde{\boldsymbol{\nu}}^T\Delta\mathbf{d}.\end{aligned} \tag{25}$$

From the definition of $\boldsymbol{\xi}$ we have $||\boldsymbol{\xi}|| \geq ||\hat{\boldsymbol{\nu}}||$ and $||\boldsymbol{\xi}|| \geq ||\tilde{\boldsymbol{\nu}}||$. According to the conditions (9)-(12), the following matrices $\mathbf{Q}_1, \mathbf{Q}_2, \mathbf{Q}_3$ and $\mathbf{Q}_4$ are positive definite

$$\begin{aligned}\mathbf{Q}_1 &\triangleq \{\mathbf{K}_1 - (1/2\beta)\Delta\mathbf{A}_1^T\mathbf{H}^{-1}\Delta\mathbf{A}_1\}, \\ \mathbf{Q}_2 &\triangleq \{\hat{\mathbf{A}}_2 - (3\beta/2)\mathbf{H}\}, \\ \mathbf{Q}_3 &\triangleq \{\mathbf{K} - (1/2\beta)\Delta\mathbf{A}_1^T\mathbf{H}^{-1}\Delta\mathbf{A}_1\}, \\ \mathbf{Q}_4 &\triangleq \{\rho\mathbf{I} - (1/2\beta)\Delta\mathbf{A}_2^T\mathbf{H}^{-1}\Delta\mathbf{A}_2\}.\end{aligned}$$

Then defining $\varrho_m \triangleq \min_{i=1,2,3,4}\{\lambda_{\min}(\mathbf{Q}_i)\}$, (25) yields

$$\begin{aligned}\dot{V} &\leq -\varrho_m(||\tilde{\boldsymbol{\eta}}||^2 + ||\tilde{\boldsymbol{\nu}}|| + ||\hat{\boldsymbol{\eta}}||^2 + ||\hat{\boldsymbol{\nu}}||^2) \\ &\quad + ||(\mathbf{K}+\mathbf{K}_1)||||\tilde{\boldsymbol{\eta}}||||\hat{\boldsymbol{\eta}}|| + ||\tilde{\boldsymbol{\nu}}||||\Delta\mathbf{d}|| - \rho_1||\hat{\boldsymbol{\nu}}||^2 \\ &\leq -\varrho_m||\boldsymbol{\xi}||^2 + ||\Delta\mathbf{d}||||\boldsymbol{\xi}|| \\ &\quad - ||(\mathbf{K}+\mathbf{K}_1)||||\tilde{\boldsymbol{\eta}}||||\hat{\boldsymbol{\eta}}||(\alpha||\hat{\boldsymbol{\nu}}||^2 - 1),\end{aligned} \tag{26}$$

Define a scalar $\sigma \in \mathbb{R}^+$ such that $0 < \sigma < \varrho_m$. The definition of $V$ in (15) yields $V \leq ||\boldsymbol{\xi}||^2$. Hence,

$$\begin{aligned}\dot{V} &\leq -(\varrho_m - \sigma)||\boldsymbol{\xi}||^2 - \sigma||\boldsymbol{\xi}||^2 + ||\Delta\mathbf{d}||||\boldsymbol{\xi}|| \\ &\quad - ||(\mathbf{K}+\mathbf{K}_1)||||\tilde{\boldsymbol{\eta}}||||\hat{\boldsymbol{\eta}}||(\alpha||\hat{\boldsymbol{\nu}}||^2 - 1) \\ &\leq -\sigma V - ||\boldsymbol{\xi}||\{(\varrho_m - \sigma)||\boldsymbol{\xi}|| - ||\Delta\mathbf{d}||\} \\ &\quad - ||(\mathbf{K}+\mathbf{K}_1)||||\tilde{\boldsymbol{\eta}}||||\hat{\boldsymbol{\eta}}||(\alpha||\hat{\boldsymbol{\nu}}||^2 - 1)\end{aligned} \tag{27}$$

Thus, one has $\dot{V} \leq -\sigma V$ when

$$\begin{aligned}\min\{||\hat{\boldsymbol{\nu}}||, ||\boldsymbol{\xi}||\} &\geq \max\{(||\Delta\mathbf{d}||/(\varrho_m - \sigma)), \sqrt{1/\alpha}\} \\ \Rightarrow ||\hat{\boldsymbol{\nu}}|| &\geq \max\{(||\Delta\mathbf{d}||/(\varrho_m - \sigma)), \sqrt{1/\alpha}\}.\end{aligned} \tag{28}$$

This affirms the UUB condition implying $\tilde{\boldsymbol{\eta}}, \tilde{\boldsymbol{\nu}}, \hat{\boldsymbol{\eta}}, \hat{\boldsymbol{\nu}} \in \mathcal{L}_\infty \Rightarrow \boldsymbol{\eta}, \boldsymbol{\nu} \in \mathcal{L}_\infty$. This concludes the proof.

**Key Performance Indicators:** From (28), an ultimate bound on the position error $\boldsymbol{\eta}$ and an upper bound of control input $\boldsymbol{\tau}$ can be computed, which can generate key performance indicators (KPI) to tune the controller.

Let $\iota \triangleq \max\{(||\Delta\mathbf{d}||/(\varrho_m - \sigma)), \sqrt{1/\alpha}\}$. From (15) we have $V \geq (1/2)||\hat{\boldsymbol{\nu}}||^2 \Rightarrow ||\hat{\boldsymbol{\nu}}|| \leq \sqrt{2V}$. Thus, from (28), we have $\dot{V} \leq -\sigma V$ when

$$\iota \leq ||\hat{\boldsymbol{\nu}}|| \leq \sqrt{2V} \Rightarrow V \geq \iota^2/2. \tag{29}$$

Therefore, defining $\iota_0 \triangleq V(0)$, one can deduce the upper bound of $V$ as

$$V \leq \max\{\iota_0,\ \iota^2/2\} \triangleq \mathcal{B}. \tag{30}$$

Utilizing the relations $||\hat{\boldsymbol{\eta}}|| \leq \sqrt{2V}$, $||\tilde{\boldsymbol{\eta}}|| \leq \sqrt{2V}$ and $||\boldsymbol{\eta}|| = ||\tilde{\boldsymbol{\eta}}|| + ||\hat{\boldsymbol{\eta}}||$, the ultimate bound $b$ on the position error $\boldsymbol{\eta}$ can be computed as follows:

$$b \in [0,\ 2\iota]. \tag{31}$$

Similarly, an upper bound on $\boldsymbol{\tau}$ can be derived from (8) as

$$\begin{aligned}&||\boldsymbol{\tau}|| = ||\mathbf{B}^{-1}\{\hat{\mathbf{A}}_1\hat{\boldsymbol{\eta}} + \hat{\mathbf{A}}_2\hat{\boldsymbol{\nu}} - \mathbf{K}_2\tilde{\boldsymbol{\eta}} - \mathbf{J}^T\hat{\boldsymbol{\eta}} - (\rho+\rho_1)\hat{\boldsymbol{\nu}}\}|| \leq \\ &\sqrt{2\mathcal{B}}||\mathbf{B}^{-1}||\left\{||\hat{\mathbf{A}}_1 - \mathbf{J}^T|| + ||\hat{\mathbf{A}}_2 - (\rho+\rho_1)|| + ||\mathbf{K}_2||)\right\}.\end{aligned} \tag{32}$$

*Remark 3.* It can be noticed from (28) and (30) that high values of $\mathbf{K}, \mathbf{K}_1, \rho$ and $\alpha$ (determined from (9)-(13)) help to reduce $\mathcal{B}$ and improve control performance. On the other hand, the upper bound (32) reveals that higher values of the above mentioned gains demands higher control effort. Thus, a designer has to make a trade-off between the positioning performance and control effort.

*Remark 4.* The DP system dynamics (1)-(2) can describe both the free-hanging and mooring stage depending on the presence of $\mathbf{F}\boldsymbol{\eta}$. Therefore, the observer-based controller (6)-(8) and the corresponding stability analysis is potentially valid under both conditions. However, it has to be noticed that when the mooring force $\mathbf{F}\boldsymbol{\eta}$ is absent, a high gain $\boldsymbol{\rho}$ might be unnecessary in view of (11): a high gain $\boldsymbol{\rho}$ might lead to an unnecessarily high control input. Therefore, one may switch to a lower gain outside the mooring phase. This would result in two different controllers for free-hanging and mooring operation which would require switching between two control structures. Such a setting

would require an ad-hoc switched based analysis, e.g. as proposed in [19] for linear switched systems or in [18] for a different DP setting. The development of a switched based analysis for the proposed controller will be the subject of future research.

## 4. VALIDATION IN SIX DOF SIMULATIONS

In order to validate the proposed DP system in a more realistic setting, a six DoF crane-vessel dynamic model with environmental disturbances will be adopted. This section presents the most important features of the simulation model for the crane-vessel system and the corresponding simulation results.

### *4.1 Simulation Model*

The simulation model is generated by WAMIT and is based on the S-175 model from MSS toolbox [20], which is valid under the following assumptions:

- The vessel is symmetrical in starboard and port.
- The bias model and the wave model are driven by zero-mean Gaussian noise.
- The vessel is moving with low velocity and low acceleration.

The various component of the simulation model are sketched in Fig. 1, and a brief description is given hereafter. The vessel dynamic model is a six DoF model with environmental disturbances, according to [21]:

$$\dot{\boldsymbol{\eta}}_f = \mathbf{R}(\phi,\theta,\psi)\boldsymbol{\nu}_f \tag{33}$$

$$(\mathbf{M}_{RB}+\mathbf{M}_A)\dot{\boldsymbol{\nu}}_f + \mathbf{C}(\boldsymbol{\nu}_{fr})\boldsymbol{\nu}_{fr} + \mathbf{D}_s\boldsymbol{\nu}_{fr} = \boldsymbol{\tau}_{wind}+\boldsymbol{\tau}_{wave}+\boldsymbol{\tau}_f+\boldsymbol{\tau}_{crane}, \tag{34}$$

where $\boldsymbol{\eta}_f = [x,y,z,\phi,\theta,\psi]^T$ is the vessel position in earth-fixed coordinate system, in which $(z,\phi,\theta)$ denote the heave position, roll and pitch angles of the vessel respectively; $\boldsymbol{\nu}_{fr} = \boldsymbol{\nu}_f - \boldsymbol{\nu}_c$ denote the relative velocity of the vessel with respect to the current velocity $\boldsymbol{\nu}_c = [u_c, v_c, w_c, 0, 0, 0]^T$, where $\boldsymbol{\nu}_f = [u,v,w,p,q,r]^T$ is the vessel velocity (all in body-fixed coordinate system); $\mathbf{R}(\phi,\theta,\psi)$ is the rotation matrix from body-fixed coordinate system to earth-fixed coordinate system; $\mathbf{M}_{RB}, \mathbf{M}_A, \mathbf{C}$ and $\mathbf{D}_s$ denote the rigid body mass matrix, added mass matrix, Coriolis terms and hydrodynamic damping terms, respectively; $\boldsymbol{\tau}_{wind}$, $\boldsymbol{\tau}_{wave}$ and $\boldsymbol{\tau}_{crane}$ are external loads from wind, wave, crane wires corresponding to external disturbance $\mathbf{d}_s$ in (1) and $\boldsymbol{\tau}_f = [\tau_x, \tau_y, \tau_z, \tau_\phi, \tau_\theta, \tau_\psi]$, where $\boldsymbol{\tau} = [\tau_x, \tau_y, \tau_\psi]$ as in (1). The terms $\mathbf{M}_{RB}$ and $\mathbf{M}_A$ are defined consistently with [21], where the latter one is based upon linear and second order potential theory. *For simulation, the sea current is considered as* $\boldsymbol{\nu}_c = [0.52, 0.30, 0, 0, 0, 0]^T$.

The environmental loads in (34) consist of wind load and wave load. The wind load could be seen as an additional air pressure to the vessel surface, leading to a force in surge, sway and moment in yaw as represented in Fig. 2. The calculations for these forces are omitted for lack of space and they can be found in [21]. The wave load consists of a first order wave load and a second order wave load.

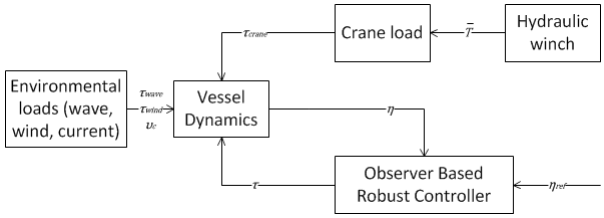


Fig. 1. Overall Simulation Model of the DP Controlled Crane Vessel

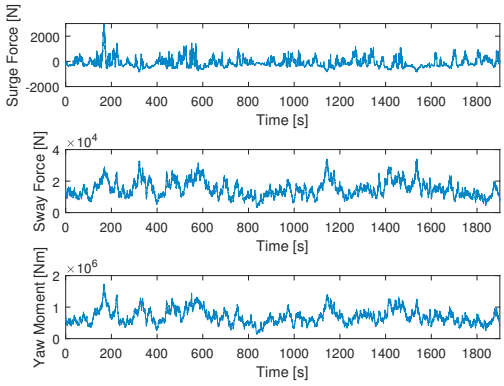


Fig. 2. Wind Load on the Vessel

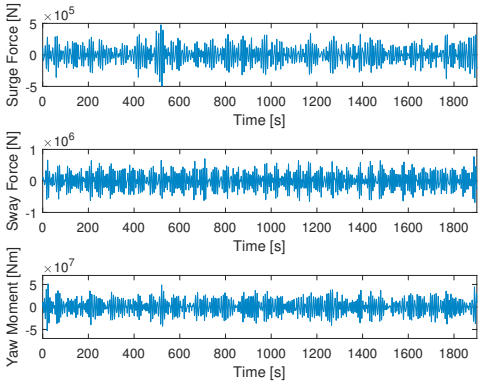


Fig. 3. First Order Wave Load on the Vessel

$$\boldsymbol{\tau}_{wave} = \boldsymbol{\tau}_{wave1} + \boldsymbol{\tau}_{wave2} \tag{35}$$

where $\boldsymbol{\tau}_{wave1}$ is a zero mean oscillation load, and $\boldsymbol{\tau}_{wave2}$ is modeled as a mean wave drift load without an oscillatory component. *In these work, the simulations are carried out under sea state* $2-3$*, when the wave has a significant wave height of* $0.5m$. The first and second order wave forces in surge, sway, and moment in yaw are shown in Fig. 3, and Fig.4. Again the calculations for these forces are omitted for lack of space and they can be found in [21].

The crane wires are modeled as an elastic wire with stiffness and damping, with a flexible length which could change with different load. The hydraulic winch controlling the force in the crane wires can be described as [22]:

$$F_{hoist} = \overline{T}/r = \eta_{hyd}\overline{Q}\Delta p/2\pi r \tag{36}$$

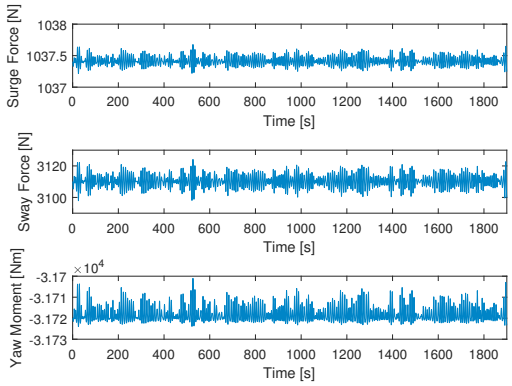


Fig. 4. Second Order Wave Load on the Vessel

where $\overline{T}$ is the hydraulic motor's torque output; $\overline{Q}$ is the inlet flow rate per revolution; $\Delta p$ is the pressure difference between the inlet flow and the outlet flow; $\eta_{hyd}$ is the efficiency of the motor; $r$ is the radius if the drum that the cable is wound on. The crane force is determined by the hydraulic motor, controlled by the following PI controller:

$$\overline{Q} = K_{hp}\delta\overline{T} + K_{hi}\int \delta\overline{T}dt \tag{37}$$

where $\delta\overline{T}$ is the difference between the desired torque and the actual torque. In line with [22], it is assumed that the pressure difference of the motor is constant and only the inlet flow rate is changing to give the desired crane force output. The resulting crane force in surge, sway and heave is represented in Fig. 5. The crane force is designed to increase from $t = 0$s to $t = 1100$s, and then decrease till $t = 1900$s. Note that such forces represent a typical mooring phase, during which the crane force increases and then decreases.

### *4.2 Simulation Results*

The nominal value $\hat{\mathbf{A}}_1$ is chosen based on the highest load during the simulation, when $\mathbf{F} = \mathbf{F}_{max}$. Thus $\hat{\mathbf{A}}_1 = 10^{-3}[2.7261\ 0\ 0;\ 0\ 2.0931\ -0.0004;\ 0\ -0.0004\ 0.0011]$; then, nominal value of $\mathbf{A}_2$ is chosen as $\hat{\mathbf{A}}_2 = 10^{-1}[0.1762\ 0\ 0;\ 0\ 1.1312\ -0.6066;\ 0\ -0.0003\ 1.3604]$ which is 91% of the actual value of $\mathbf{A}_2$. Other parameters involved in the simulation are chosen as: $\mathbf{M} = 10^{10}[0.0026\ 0\ 0;\ 0\ 0.0033\ 0.0015;\ 0\ 0.0015\ 6.5209]$; the upper bound of disturbance is chosen as $\Delta\mathbf{d} = [0.1948,\ 1.4940,\ 0.0012]^T$. The upper bounds of the perturbation $\Delta\mathbf{A}_1$ and $\Delta\mathbf{A}_2$ are selected to be 10% and 100% of $\hat{\mathbf{A}}_1$ and $\hat{\mathbf{A}}_2$, respectively. The various control design parameters are selected as $\alpha = 2, \beta = 1$ and $\mathbf{H} = \Delta\mathbf{A}_2$. Consequently, other control gains turn out to be: $\mathbf{K} = \mathbf{K}_1 = 0.0023\mathbf{I}$; $\rho = 1.6670$; $\rho_1(t) = 0.0093||\hat{\boldsymbol{\eta}}(t)||||\tilde{\boldsymbol{\eta}}(t)||$.

Under the influence of a time-varying crane force (Fig. 5), the performance of the proposed controller are shown in Fig. 6 in terms of the simulated vessel's north, east position and yaw movement. It is evident that the vessel maintains required position with small offsets in the north and east position.

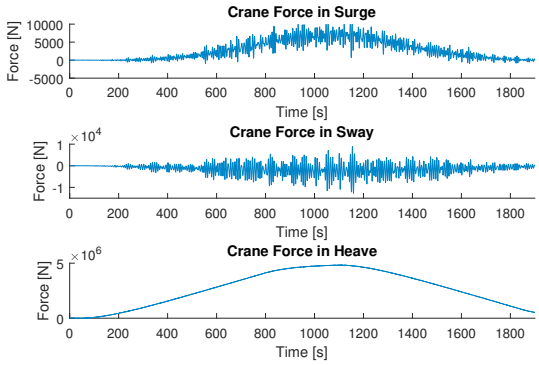


Fig. 5. Crane Force on the DP Controlled Vessel

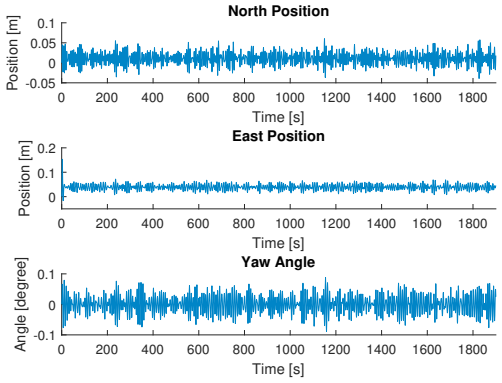


Fig. 6. Position of the DP Controlled Vessel

Table 1. Comparison Between Different Control Methods

| Control Method | | PID | Proposed Controller |
|---|---|---|---|
| Root Mean Square | North$[m]$ | 0.05 | 0.02 |
| | East$[m]$ | 0.13 | 0.04 |
| | $\psi[^\circ]$ | 0.27 | 0.03 |
| Maximum Offset | North$[m]$ | 0.24 | 0.06 |
| | East$[m]$ | 0.42 | 0.15 |
| | $\psi[^\circ]$ | 0.64 | 0.09 |

To further highlight the effectiveness of the proposed design, another simulation is carried out using a traditional PID controller in conjunction with the observer (6)-(7). For this simulation, the PID gains are selected as $\mathbf{K}_p = 10^6 diag(7, 15, 50)$, $\mathbf{K}_i = 10^3 diag(5, 5, 10)$, $\mathbf{K}_d = 10^4 diag(5, 5, 10)$, based on the general guidelines followed in the industry for such vessels [25]. It is evident from the comparative results between the PID and the proposed controller in Table 1, that the proposed controller provides better performance comparing to traditional PID controller in all three directions.

## 5. CONCLUSION AND FUTURE WORK

In this work, an observer based robust controller was presented for the position control of large-scale heavy lift vessels. The observer was specifically used to attenuate the high frequency vessel movement caused by environmental load. Additionally, use of only position feedback in the control law reduces the vulnerability toward high frequency velocity noise. The controller was designed to

be robust against model uncertainty in damping matrix, mooring force and external disturbances. The closed-loop system was shown to be UUB and the effectiveness of the proposed scheme was verified in simulation under changing mooring force and environmental load.

Note that in heavy lift vessels, the mass matrix is subject to relatively small uncertainty as compared to mooring and damping terms [2]. Hence, the proposed controller utilized, precise knowledge of mass matrix. Nevertheless, the added mass is unknown in practice and causes model imperfection. Therefore, an important future direction would be to consider perturbation in mass matrix for control design including thruster dynamics.

## REFERENCES


[1] Flint J, Stephens R. Dynamic positioning for heavy lift applications. In: *Dynamic Positioning Conference*, 2008, Huston, Texas, USA.

[2] Ellermann K, Kreuzer E and Markiewicz M. Nonlinear dynamics of floating cranes. In: *Nonlinear Dynamics*. 2002 Jan 1;27(2).

[3] Watters AJ, Moore DJ and McGill LS. Dynamics of offshore cranes. In: *Offshore Technology Conference*. 1980 May, Houston, Texas, USA.

[4] Osiński M, Maczyński A and Wojciech S. The influence of ship's motion in regular wave on dynamics of an offshore crane. In: *Archive of Mechanical Engineering*. 2004

[5] Vorhölter H, Hatecke H and Feder DF. Design study of floating crane vessels for lifting operations in the offshore wind industry. In: *Proceedings of '15 International Marine Design Conference*. 2015 May:1-13.

[6] Ye J, Godjevac M and el Amam E. Position control of crane vessel during offshore installations: Using adaptive and robust control methods. In: *International Conference on System Theory, Control and Computing*. Sinaia, 2017:17-22.

[7] Ye J, Godjevac M, Baldi S, Hopman H. Joint estimation of vessel position and mooring stiffness during offshore crane operations. In: *Automation in Construction*. 2019 May 1;101:218-26.

[8] Ngo QH, Hong KS. Sliding-mode antisway control of an offshore container crane. In: *IEEE/ASME Transactions on Mechatronics*. 2012 Apr;17(2):201-9

[9] Sun N, Fang Y, Chen H and He B. Adaptive nonlinear crane control with load hoisting/lowering and unknown parameters: design and experiments. In: *IEEE/ASME Transactions on Mechatronics*, 2015 Oct;20(5):2107-2119.

[10] Küchler S, Mahl T, Neupert J, Schneider K and Sawodny O. Active control for an offshore crane using prediction of the vessel's motion. In: *IEEE/ASME Transactions on Mechatronics*, 2011 Apr;16(2):297-309.

[11] Messineo S, Serrani A. Offshore crane control based on adaptive external models. In: *Automatica*. 2009 Nov 1;45(11):2546-56.

[12] Du J, Hu X, Krstic M and Sun Y. Dynamic positioning of ships with unknown parameters and disturbances. In: *Control Engineering Practice*, 2018;76:22-30.

[13] Hu Z, Du J. Robust nonlinear control design for dynamic positioning of marine vessels with thruster system dynamics. In: *Nonlinear Dynamics*, 2018;94:365-376.

[14] Wang Y, Tuo a Y, Yang SX, Biglarbegian M and Fu M. Reliability-based robust dynamic positioning for a turret-moored floating production storage and offloading vessel with unknown time-varying disturbances and input saturation. In: *ISA Transactions*, 2018;78:66-79.

[15] Yu WZ, Xu HZ and Feng H. Robust adaptive fault-tolerant control of dynamic positioning vessel with position reference system faults using backstepping design. In: *International Journal of Robust and Nonlinear Control*, 2018;28:403-415.

[16] Sun Z, Zhang G, Qiao L and Zhang W. Robust adaptive trajectory tracking control of underactuated surface vessel in fields of marine practice. In: *Journal of Marine Science and Technology*, 2018.

[17] Grovlen A, Fossen TI. Nonlinear control of dynamic positioned ships using only position feedback: an observer backstepping approach. In: *IEEE Conference on Decision and Control*, 1996.

[18] Brodtkorb AH, Værnø SA, Teel AR, Sørensen AJ and Skjetne R. Hybrid controller concept for dynamic positioning of marine vessels with experimental results. In: *Automatica*, 2018;93:489-497.

[19] Yuan S, De Schutter B and Baldi S. Robust adaptive tracking control of uncertain slowly switched linear systems. In: *Nonlinear Analysis: Hybrid Systems*, 2018;27:1-12.

[20] Fossen TI, Perez T. Marine Systems Simulator (MSS). http://www.marinecontrol.org.

[21] Fossen TI. *Handbook of marine craft hydrodynamics and motion control*. John Wiley & Sons; 2011 May 23

[22] Brater EF, King HW, Lindell JE and Wei CY. *Handbook of hydraulics for the solution of hydraulic engineering problems (Vol. 7)*. New York: McGraw-Hill; 1996

[23] Khalil H. *Noninear systems*. Prentice Hall; 2002.

[24] Roy S. and Kar IN. Adaptive robust tracking control of a class of nonlinear systems with input delay. In: *Nonlinear Dynamics*, 2017;85(2):1127-1139.

[25] Ye J. *Dynamic Positioning during Heavy Lift Operations: Using fuzzy control techniques, Nonlinear Observer and H-Infinity Method Separately to Obtain Stable DP Systems for Heavy Lift Operations*. (2016). Available from repository.tudelft.nl.